A generalized distribution interpolated between the exponential and power law distributions and applied to the walking data of the pill bug (*Armadillidium vulgare*)

Shuji Shinohara[1*], Hiroshi Okamoto[1], Toru Moriyama[2], Yoshihiro Nakajima[3], Takaharu Shokaku[4], Akika Utsumi[2], Ung-il Chung[1]

1 Department of Bioengineering, Graduate School of Engineering, The University of Tokyo, Tokyo, Japan

2 Faculty of Textile Science, Shinshu University, Ueda, Japan

3 Graduate School of Economics, Osaka City University, Osaka, Japan

4 Department of Network Design, Meiji University, Tokyo, Japan

* Corresponding author

E-mail: shinohara@bioeng.t.u-tokyo.ac.jp (SS)

AUTHOR CONTRIBUTIONS STATEMENT

Shuji Shinohara: conceptualization, formal analysis, methodology, software, writing — original draft preparation, funding acquisition. Hiroshi Okamoto: Conceptualization, Methodology, writing—review, and Editing Toru Moriyama: Resources, data curation, writing—review, and editing. Yoshihiro Nakajima: Writing—review, and editing. Takaharu Shokaku: Resources, data curation, writing—review, and editing. Akika Utsumi: Resources, data curation, writing—review, and editing. Ung-il Chung: Writing—review and editing, supervision, and project administration.

Abstract

To determine whether the walking pattern of an organism is a Lévy walk or a Brownian walk, it has been compared whether the frequency distribution of linear step lengths follows a power law distribution or an exponential distribution. However, there are many cases where actual data cannot be classified into either of these categories. In this paper, we propose a general distribution that includes the power law and exponential distributions as special cases. This distribution has two parameters: One represents the exponent, similar to the power law and exponential distributions, and the other is a shape parameter representing the shape of the distribution. By introducing this distribution, an intermediate distribution model can be interpolated between the power law and exponential distributions. In this study, the proposed distribution was fitted to the frequency distribution of the step length calculated from the walking data of pill bugs. The autocorrelation coefficients were also calculated from the time-series data of the step length, and the relationship between the shape parameter and time dependency was investigated. The results showed that individuals whose step-length frequency distributions were closer to the power law distribution had stronger time dependence.

Keywords

Power law distribution, Exponential distribution, generalized distribution, Weibull distribution, Time dependence of step length, pill bug, Random walk

Introduction

Lévy walks are found in the migratory behavior of organisms at various levels, from bacteria and T cells to humans [1–6]. Lévy walks are a type of random walk in which the frequency of occurrence of a linear step length l follows a power law distribution $p(l) \sim l^{-\mu}, 1 < \mu \leq 3$. Compared to the Brownian walk, which is also a type of random walk (characterized by an exponential distribution $p(l) \sim e^{-\lambda l}$ of the frequency of occurrence of step length l), the Lévy walk is characterized by the occasional appearance of linear movements over very long distances, and why such patterns occur in biological migration has attracted attention [7].

To determine whether the gait pattern is a Lévy walk or a Brownian walk, a comparison is made concerning whether the frequency distribution of the linear step length follows a power law distribution or an exponential distribution [5,8–12]. In the comparison, the range of step lengths to be analyzed and the parameters of the model that best fit the data in that range, that is, the exponents μ and λ, are first calculated. The maximum likelihood estimation method is generally used to estimate the parameters. Next, a comparison is made to determine which model fits better, the power law distribution model, or the exponential distribution model. For comparison, Akaike information criteria weights (AICw), which considers the likelihood and number of parameters, are often used [11,12]. To verify whether the model fits the observed data, Clauset et al. [10] proposed goodness-of-fit tests based on the Kolmogorov-Smirnov (KS) statistic. In this way, judgments have been made as to whether the observed data follow a power law distribution or an exponential distribution model, but many actual data cannot be classified as either [3].

In this paper, we propose a general distribution such that the power law and exponential distributions are included as special cases. This distribution has two parameters: One represents the exponent, similar to the power law and exponential distributions, and the other is a shape parameter representing the shape of the distribution. In this distribution, if the shape parameter is set to a specific value, it represents the power law distribution, and if it is set to another specific value, it represents an exponential distribution. By introducing this distribution, distributions that are intermediate between the power law and exponential distributions can be modeled. In this study, the proposed distribution was fitted to the walking data of pill bugs collected by Shokaku et al. [3] as specific observation data. Differently expressed, we estimated the exponent and shape parameters that best fit the observed data.

It has been asserted that there is a time dependency in the time series of the step length in human mobility behavior. For example, Wang et al. [13], Rhee et al. [14], and Zhao et al. [15] demonstrated that the temporal variation of step length is autocorrelated, which means that there is a trend in the time variation of step length, such that short (long) steps are followed by short (long) steps. In addition, it has been emphasized that the time dependence of step length is related to the frequency distribution of the step length following a power law distribution [13].

In this study, to investigate the time dependence of the walking data of the pill bugs described above, we calculated the autocorrelation coefficient between the time series l_t of the step length and the time series $l_{t+\tau}$ with time lag τ. When τ=0, the autocorrelation coefficient is 1 because the two time series are identical. Conversely, when τ>0, any random walk such as the Lévy walk or Brownian walk is theoretically uncorrelated. We investigated the relationship between the autocorrelation coefficient calculated from the time-series data of the linear step length and the shape parameter of the frequency distribution of the linear step length. The results showed that individuals whose frequency distributions were closer to the power law distribution than to the exponential distribution tended to show stronger time dependence.

Methods

A distribution interpolated between the exponential and power law distributions

In this section, we propose a general distribution that includes exponential and power-law distributions as special cases. First, let us consider the process of elongating the persistence length. This length can be a spatial distance or a time interval. For example, consider a process in which an organism continues to move in a straight line and reaches a distance of l, and then moves in the same straight line by a dl, for the total straight-line distance to increase to $l+dl$. As a discrete example, consider the process of tossing a coin and getting "heads" l times, then getting "heads" again, and extending the period of consecutive "heads" to l+1 times.

Suppose that the probability of length l occurring is represented by $p(l)$. Because l is a length, let $l \geq 0$. Because $p(l)$ is a probability distribution, it satisfies $\int_0^\infty p(l)dl = 1$. Let us also denote by $P(l)$ the complementary cumulative frequency distribution (CCDF) in which lengths greater than or equal to l occur. That is,

$$P(l) = \int_l^\infty p(x)dx \qquad (1)$$

Based on this definition, $P(0) = \int_0^\infty p(x)dx = 1$ is valid. Similarly, from the definition, the following relationship holds between $p(l)$ and $P(l)$.

$$p(l) = -\frac{dP(l)}{dl} \qquad (2)$$

We denote $f(l)$ the probability that the length l will extend to $l+dl$. $f(l)$ can be expressed by:

$$f(l) = \frac{P(l+dl)}{P(l)} \qquad (3)$$

In contrast, the probability that length l is reached and ends at l is denoted by $g(l)$. $g(l)$ can be expressed using $p(l)$ and, $P(l)$ as follows:

$$g(l) = \frac{p(l)}{P(l)}dl \qquad (4)$$

Here, an interval of length l can either extend further from l or end at l, therefore, $f(l)+g(l)=1$ holds. To consider the elongation process in the discrete case, that is, when dl=1, let us consider a situation in which a coin is tossed repeatedly. We assume a situation in which the probability of “heads” in a coin toss is not constant, but varies depending on the number of times the same side appears consecutively. For example, after three consecutive "heads", the probability that the next is also "heads" is represented by $f(3)$. Conversely, the probability that the next is "tails" is expressed as $g(3)=1\text{-}f(3)$.

The CCDF that the same side will continue for $l+1$ or more consecutively is expressed as follows:

$$P(l+1)=\prod_{i=1}^{l} f(i)=f(l)\prod_{i=1}^{l-1} f(i)=f(l)P(l) \qquad (5)$$

The probability that the same side continues consecutively for l times, that is, the probability of length l occurring, is expressed as follows:

$$p(l)=g(l)\prod_{i=1}^{l-1} f(i)=g(l)P(l) \qquad (6)$$

Now, let us consider Brownian and Lévy walks. For the Brownian walk, the probability of a step length l occurring and its CCDF is represented by the following exponential distribution with an exponent β.

$$\begin{cases} p(l)\propto \beta e^{-\beta l} \\ P(l)\propto e^{-\beta l} \end{cases} \qquad (7)$$

Conversely, for the Lévy walk, the probability of the occurrence of a step length l and the CCDF is expressed by the following power law distribution with the exponent β.

$$\begin{cases} p(l)\propto \beta l^{-(\beta+1)} \\ P(l)\propto l^{-\beta} \end{cases} \qquad (8)$$

If the change rate at length l is defined as $\gamma(l)=\dfrac{g(l)}{dl}=\dfrac{p(l)}{P(l)}$, the change rates of the Brownian walk and the Lévy walk can be expressed as follows:

$$\gamma(l)=\frac{p(l)}{P(l)}=\frac{\beta e^{-\beta l}}{e^{-\beta l}}=\beta=\beta l^{-0} \qquad (9)$$

$$\gamma(l)=\frac{p(l)}{P(l)}=\frac{\beta l^{-(\beta+1)}}{l^{-\beta}}=\beta l^{-1} \qquad (10)$$

We now define the generalized rate of change to include the Brownian and Lévy walk as a special case, as follows:

$$\gamma(l)=\frac{p(l)}{P(l)}=\beta l^{-\alpha} \qquad (11)$$

The case of α=0 corresponds to the change rate of the Brownian walk, and the case of α=1 corresponds to the change rate of the Lévy walk.

Equation (11) can be written as $\gamma(l)=-\frac{dP(l)}{dl}\Big/P(l)=\beta l^{-\alpha}$, and solving it for $P(l)$ yields the following solution:

$$P(l)=\exp\left(-\frac{\beta}{-\alpha+1}l^{-\alpha+1}\right) \qquad (12)$$

If we put $m=-\alpha+1$, then $P(l)$ is expressed as follows:

$$P(l)=\exp\left(-\frac{\beta}{m}l^{m}\right) \qquad (13)$$

The probability $p(l)$ of step length l occurring can be written as follows, using equation (2).

$$\begin{aligned} p(l)&=-\frac{dP(l)}{dl} \\ &=\beta l^{m-1}\exp\left(-\frac{\beta}{m}l^{m}\right) \end{aligned} \qquad (14)$$

In addition, because -α=m-1, the change rate in equation (11) can be written as follows:

$$\gamma(l)=\beta l^{m-1} \qquad (15)$$

Let us consider the meanings of m and β. As can be seen from equation (15), the change rate becomes smaller as the value of l increases, since m-1<0 holds in the range of m<1. Conversely, the longer this persists, the greater the probability that it will continue the next time. When m>1, the change rate increases as l increases. Differently put, the longer the value of l, the higher is the change rate. When m=1, the change rate is a constant value β, regardless of the value of l. Thus, m is a parameter that controls how the length of l, or the past history of how long the same condition has lasted, is taken into account.

Conversely, for β, if l and m are fixed, the larger β becomes, the higher the change rate becomes. Otherwise expressed, β is a parameter that controls the magnitude of the change rate.

For $m = 1$, equation (14) is expressed as follows:

$$p(l) = \beta \exp(-\beta l) \qquad (16)$$

Put differently, it represents an exponential distribution of the exponent -β. Conversely, when $m = 0$, equation (14) cannot be defined because it involves division by zero. However, when m is sufficiently close to zero, this distribution can be approximated using the Maclaurin expansion, $l^m \approx 1 + m \log l$ as follows:

$$\begin{aligned}
p(l) &= \beta l^{m-1} \exp\left(-\frac{\beta}{m} l^m\right) \\
&\approx \beta l^{m-1} \exp\left(-\frac{\beta}{m}(1 + m \log l)\right) \\
&= \beta l^{m-1} \exp\left(-\frac{\beta}{m} - \beta \log l\right) \\
&= \beta l^{m-1} \exp\left(-\frac{\beta}{m}\right) \exp(-\beta \log l) \\
&= \beta l^{m-1} \exp\left(-\frac{\beta}{m}\right) \exp\left(\log l^{-\beta}\right) \\
&= \beta l^{m-1} \exp\left(-\frac{\beta}{m}\right) l^{-\beta} \\
&= \beta \exp\left(-\frac{\beta}{m}\right) l^{-(\beta - m + 1)} \\
&\approx \beta \exp\left(-\frac{\beta}{m}\right) l^{-(\beta + 1)} \qquad (17)
\end{aligned}$$

If we set $Z = \frac{1}{\beta} \exp\left(\frac{\beta}{m}\right)$ as the normalization constant, equation (17) can be rewritten as follows:

$$p(l) \approx \frac{1}{Z} l^{-(\beta+1)} \qquad (18)$$

Otherwise expressed, equation (14) represents the power law distribution of the exponent –(β+1) as an approximation. Thus, equation (14) can be said to be a distribution that includes not only the exponential distribution but also the power law distribution as a special case, albeit as an approximation. Therefore, in this study, for convenience, the distribution of equation (14) is named the generalized distribution (GE). Furthermore, parameter m is called the shape parameter in the sense that it represents the shape of the distribution.

Relationship between the generalized distribution (GE) and Weibull distribution

We discuss the relationship between the GE and the Weibull distribution [16]. The Weibull distribution is used to describe the degradation phenomenon and lifetime of a component statistically, and is expressed as follows:

$$p(l) = \frac{m}{\eta}\left(\frac{l}{\eta}\right)^{m-1} \exp\left(-\left(\frac{l}{\eta}\right)^{m}\right) \qquad (19)$$

Here, η is the scale parameter. Conversely, m is a parameter that determines the shape of the distribution and is called the shape parameter. The CCDF of the Weibull distribution is expressed as

$$P(l) = \exp\left(-\left(\frac{l}{\eta}\right)^{m}\right) \qquad (20)$$

In the Weibull distribution, if we set m=1 and η=1/λ, an exponential distribution with an exponent λ is obtained as follows:

$$p(l) = \frac{m}{\eta}\left(\frac{l}{\eta}\right)^{m-1} \exp\left(-\left(\frac{l}{\eta}\right)^{m}\right) = \frac{1}{\eta}\exp\left(-\frac{l}{\eta}\right) = \lambda\exp(-\lambda l) \qquad (21)$$

In addition, if m=2 and $\eta = \sqrt{2}\sigma$, the Weibull distribution represents the Rayleigh distribution as shown below:

$$p(l)=\frac{m}{\eta}\left(\frac{l}{\eta}\right)^{m-1}\exp\left(-\left(\frac{l}{\eta}\right)^{m}\right)=\frac{2}{\eta}\left(\frac{l}{\eta}\right)\exp\left(-\left(\frac{l}{\eta}\right)^{2}\right)=\frac{l}{\sigma^{2}}\exp\left(-\frac{l^{2}}{2\sigma^{2}}\right) \quad (22)$$

Thus, the Weibull distribution includes exponential and Rayleigh distributions as special cases. Let us consider the relationship between the Weibull distribution and GE. If we set $\eta=(m/\beta)^{\frac{1}{m}}$, equation (19) can be transformed as follows:

$$\begin{aligned}
p(l)&=\frac{m}{\eta}\left(\frac{l}{\eta}\right)^{m-1}\exp\left(-\left(\frac{l}{\eta}\right)^{m}\right)\\
&=\frac{m}{\eta^{m}}l^{m-1}\exp\left(-\frac{l^{m}}{\eta^{m}}\right)\\
&=\frac{m}{\left((m/\beta)^{\frac{1}{m}}\right)^{m}}l^{m-1}\exp\left(-\frac{l^{m}}{\left((m/\beta)^{\frac{1}{m}}\right)^{m}}\right) \quad (23)\\
&=\frac{m}{(m/\beta)}l^{m-1}\exp\left(-\frac{l^{m}}{(m/\beta)}\right)\\
&=\beta l^{m-1}\exp\left(-\frac{\beta}{m}l^{m}\right)
\end{aligned}$$

Expressed differently, it is consistent with GE. However, these two are not equivalent. As shown in equation (16), when m=1, GE represents an exponential distribution. In addition, if m=2 and $\beta=1/\sigma^{2}$, then GE represents the Rayleigh distribution.

$$p(l)=\beta l\exp\left(-\frac{\beta}{2}l^{2}\right)=\frac{l}{\sigma^{2}}\exp\left(-\frac{l^{2}}{2\sigma^{2}}\right) \quad (24)$$

Thus, for m=1 and m=2, the GE is similar to the Weibull distribution. However, when m is close to zero, a difference is observed. When m is close to zero, the Weibull distribution can be approximated using the Maclaurin expansion $l^{m}\approx 1+m\log l$ as follows:

$$
\begin{aligned}
p(l) &= \frac{m}{\eta}\left(\frac{l}{\eta}\right)^{m-1}\exp\left(-\left(\frac{l}{\eta}\right)^{m}\right)\\
&\approx \frac{m}{\eta^m} l^{m-1}\exp\left(-\frac{1+m\log l}{\eta^m}\right)\\
&= \frac{m}{\eta^m} l^{m-1}\exp\left(-\frac{1}{\eta^m}-\frac{m}{\eta^m}\log l\right)\\
&= \frac{m}{\eta^m} l^{m-1}\exp\left(-\frac{1}{\eta^m}\right)\exp\left(-\frac{m}{\eta^m}\log l\right)\\
&= \frac{m}{\eta^m} l^{m-1}\exp\left(-\frac{1}{\eta^m}\right)\exp\left(\log l^{-\frac{m}{\eta^m}}\right)\\
&= \frac{m}{\eta^m} l^{m-1}\exp\left(-\frac{1}{\eta^m}\right) l^{-\frac{m}{\eta^m}}\\
&= \frac{m}{\eta^m}\exp\left(-\frac{1}{\eta^m}\right) l^{m-1-\frac{m}{\eta^m}}\\
&\approx \frac{m}{\eta^m}\exp\left(-\frac{1}{\eta^m}\right) l^{-1}
\end{aligned}
\tag{25}
$$

If we set $Z = \frac{\eta^m}{m}\exp\left(\frac{1}{\eta^m}\right)$ as the normalization constant, equation (25) can be rewritten as follows:

$$p(l) \approx \frac{1}{Z} l^{-1} \tag{26}$$

When m is sufficiently close to zero, the Weibull distribution can be approximated as a power law distribution with an exponent of -1. Put differently, the Weibull distribution only represents the power law distribution with the exponent -1, regardless of the value of η. Conversely, GE can approximate the power law distribution of any exponent with $-(\beta+1)$as a parameter, as shown in equation (18).

Parameter Estimation

The GE has two parameters: m and β. In this section, we describe a method for estimating these parameters from the observed data. The first objective of this section is to find the minimum $\hat{l}_{\min}$ and maximum $\hat{l}_{\max}$ of the observed data that should be fitted to the GE model. The second objective is to find the parameters

$\widehat{m}$ and $\widehat{\beta}$ of the GE model that best fit the data in the range $\hat{l}_{\min} \le l \le \hat{l}_{\max}$. Suppose we are given N observed data $D = \{l_1, l_2, \cdots, l_N\}$ in the range of $l_{\min} \le l \le l_{\max}$. The model for the data must be satisfied $\int_{l_{\min}}^{l_{\max}} p(l)dl = 1$. For this reason, we multiply equation (14) by a constant term and redefine the GE model as follows:

$$\begin{aligned} p(l;\beta,m,l_{\min},l_{\max}) &= \frac{1}{\int_{l_{\min}}^{l_{\max}} p(x)dx} p(l) \\ &= \frac{1}{\int_{l_{\min}}^{l_{\max}} \beta x^{m-1} \exp\left(-\frac{\beta}{m} x^m\right) dx} \beta l^{m-1} \exp\left(-\frac{\beta}{m} l^m\right) \\ &= \frac{1}{\exp\left(-\frac{\beta}{m} l_{\min}{}^m\right) - \exp\left(-\frac{\beta}{m} l_{\max}{}^m\right)} \beta l^{m-1} \exp\left(-\frac{\beta}{m} l^m\right) \end{aligned} \quad (27)$$

When the observed data are discrete, such as natural numbers, they are defined as follows:

$$\begin{aligned} p(l;\beta,m,l_{\min},l_{\max}) &= \frac{1}{\sum_{i=l_{\min}}^{l_{\max}} p(i)} p(l) \\ &= \frac{1}{\sum_{i=l_{\min}}^{l_{\max}} \beta i^{m-1} \exp\left(-\frac{\beta}{m} i^m\right)} \beta l^{m-1} \exp\left(-\frac{\beta}{m} l^m\right) \end{aligned} \quad (28)$$

In addition, because the CCDF of $p(l;\beta,m,l_{\min},l_{\max})$ must satisfy $P(l_{\min}) = 1$, we redefine it as follows:

$$P(l;\beta,m,l_{\min},l_{\max}) = \frac{\exp\left(-\frac{\beta}{m} l^m\right) - \exp\left(-\frac{\beta}{m} l_{max}{}^m\right)}{\exp\left(-\frac{\beta}{m} l_{\min}{}^m\right) - \exp\left(-\frac{\beta}{m} l_{max}{}^m\right)} \quad (29)$$

When the observed data is discrete, the CCDF is defined as follows:

$$P(l;\beta,m,l_{\min},l_{\max}) = \frac{\sum_{i=l}^{l_{\max}} \beta i^{m-1} \exp\left(-\frac{\beta}{m} i^m\right)}{\sum_{i=l_{\min}}^{l_{\max}} \beta i^{m-1} \exp\left(-\frac{\beta}{m} i^m\right)} \quad (30)$$

The log-likelihood of the observed data D was calculated using the following equation (27) as follows:

$$
\begin{aligned}
\ln L(\beta, m; l_{\min}, l_{\max}) &= \sum_{i=1}^{N} \ln p(l_i; \beta, m, l_{\min}, l_{\max}) \\
&= \sum_{i=1}^{N} \left(-\ln\left(\exp\left(-\frac{\beta}{m} l_{\min}{}^{m}\right) - \exp\left(-\frac{\beta}{m} l_{\max}{}^{m}\right)\right) + \ln\beta + \ln l_i{}^{m-1} + \ln\exp\left(-\frac{\beta}{m} l_i{}^{m}\right)\right) \\
&= \sum_{i=1}^{N} \left(-\ln\left(\exp\left(-\frac{\beta}{m} l_{\min}{}^{m}\right) - \exp\left(-\frac{\beta}{m} l_{\max}{}^{m}\right)\right) + \ln\beta + (m-1)\ln l_i - \frac{\beta}{m} l_i{}^{m}\right) \\
&= \sum_{i=1}^{N} \left(C + (m-1)\ln l_i - \frac{\beta}{m} l_i{}^{m}\right) \\
&= NC + \sum_{i=1}^{N} \left((m-1)\ln l_i - \frac{\beta}{m} l_i{}^{m}\right)
\end{aligned}
\qquad (31)
$$

Here $C = -\ln\left(\exp\left(-\frac{\beta}{m} l_{\min}{}^{m}\right) - \exp\left(-\frac{\beta}{m} l_{\max}{}^{m}\right)\right) + \ln\beta$. The log-likelihood when the observed data are discrete can be replaced by $C = -\ln\left(\sum_{i=l_{\min}}^{l_{\max}} \beta i^{m-1} \exp\left(-\frac{\beta}{m} i^{m}\right)\right) + \ln\beta$.

The model parameters that best fit the observed data are $\widehat{m}$ and $\widehat{\beta}$, which maximize the log-likelihood. In this paper, m varies from 0.01 to 1.0 and β from 0.01 to 4.0 in increments of 0.01, and the parameters $\widehat{m}$ and $\widehat{\beta}$ for which equation (31) is maximized are obtained numerically. When $m = 0$, equation (31) cannot be defined; therefore, we set the number sufficiently close to 0, $m = 0.01$.

To evaluate the model's goodness of fit to the observed data, we used the Kolmogorov-Smirnov statistic $D(l_{\min}, l_{\max})$, which represents the distance between the CCDF, $S(l; l_{\min}, l_{\max})$, calculated from the observed data D and the theoretical CCDF expressed in equation (29) or equation (30).

$$
D(l_{\min}, l_{\max}) = \max_{l_{\min} \le l \le l_{\max}} \left| S(l; l_{\min}, l_{\max}) - P\left(l; \widehat{\beta}, \widehat{m}, l_{\min}, l_{\max}\right)\right| \qquad (32)
$$

In this paper, let $\hat{l}_{\max}$ be the maximum $l_{\max}$ of the observed data.

If $l_{\max} = \hat{l}_{\max}$, then $D\left(l_{\min}, \hat{l}_{\max}\right)$ can be considered as a function of $l_{\min}$. $\hat{l}_{\min}$, which minimizes $D\left(l_{\min}, \hat{l}_{\max}\right)$, is numerically calculated from within the observed data. That is,

$$\hat{l}_{\min} = \underset{l \in D}{\arg\min}\, D\left(l, \hat{l}_{\max}\right) \qquad (33)$$

As shown above, $\hat{l}_{\min}$, $\widehat{m}$, and $\widehat{\beta}$ can be obtained numerically using equations (31) and (33).

Autocorrelation coefficient

Suppose we are given T time-series data $\left(l_1, l_2, \cdots, l_T\right)$. In this case, the autocorrelation coefficient $r(\tau)$ with time lag τ is expressed as follows:

$$\begin{aligned} r(\tau) &= \frac{\sum_{t=1}^{T-\tau}\left(l_t - \bar{l}_{1,T-\tau}\right)\left(l_{t+\tau} - \bar{l}_{1+\tau,T}\right)}{\sqrt{\sum_{t=1}^{T-\tau}\left(l_t - \bar{l}_{1,T-\tau}\right)^2}\sqrt{\sum_{t=1}^{T-\tau}\left(l_{t+\tau} - \bar{l}_{1+\tau,T}\right)^2}} \\ \bar{l}_{1,T-\tau} &= \frac{\sum_{t=1}^{T-\tau} l_t}{T-\tau} \\ \bar{l}_{1+\tau,T} &= \frac{\sum_{t=1}^{T-\tau} l_{t+\tau}}{T-\tau} \end{aligned} \qquad (34)$$

When τ=0, we take the correlation coefficient between the same time-series data $r(0)$=1. We calculated the autocorrelation coefficients of the time-series data of linear step length to investigate the time dependence of the pill bugs' walking data. In this study, the autocorrelation coefficient was obtained in the range of τ = 1–100. The autocorrelation coefficients for every individual are averaged from $r(1)$ to $r(100)$ and are expressed as $\bar{r}$.

$$\bar{r} = \frac{\sum_{\tau=1}^{100} r(\tau)}{100} \qquad (35)$$

The programs for the parameter estimation and autocorrelation coefficient calculation described above were developed using C++. The compiler was MinGW 8.1.0 64-bit for C++ [17]. The Qt library (Qt version

Qt 5.15.2 MinGW 64-bit) was also used for development [18].

Statistical analyses

Wilcoxon's rank sum test was used to test the difference in means. For all analyses statistical significance was set at $p < 0.01$. The following analysis was performed using the R 3.6.1 statistical software (2019-07-05) [19] unless otherwise specified. We used the R packages of exactRankTests version 0.8.31 for the Wilcoxon rank sum test. The operating system used was Windows 10.

Application

We applied the method described above to the pill bug's gait data. It is known that pill bugs have a habit termed turn alternation, following which they turn to the right (left), left (right), and so on [20]. The mechanism underlying turn alternation is assumed to be based primarily on proprioceptive information from the previous turn and arises from bilaterally asymmetrical leg movements that occur when turning [21]. During one turn, the outer-side legs travel further than the inner ones. After completing the turn, the relatively rested inner-side legs exert more influence on subsequent movements than the outer-side ones and bias the animal to turn in the opposite direction at the next step.

By alternating turns, pill bugs can maintain a straight course to avoid an obstacle. Moving in a straight course is considered the most adaptive strategy when precise information about environmental resources or hazards is absent [22]. However, when pill bugs were examined in successive T-mazes, they sometimes turned in the same direction as they had at the previous junction (turn repetition). For example, in an experiment on 12 pill bugs using 200 successive T-mazes (for approximately 30 min), three individuals maintained a high rate of turn alternation, four a low rate, and the remaining five spontaneously increased and decreased the rate [23]. Why some pill bugs did not maintain a high rate of turn alternation, that is, generate turn repetition at a rate other than low, is still unclear.

Shokaku et al. developed an automatic turntable-type multiple T-maze device to observe the appearance of turn alternation and turn repetition in pill bugs over a long period and to investigate the effects of these turns on gait patterns [3]. This is a virtually infinite T-maze that uses a turntable. The pill bug turns to the left or right at a T-junction, goes straight ahead, and then crosses another T-junction, and so on. Using this device, Shokaku et al. observed 34 pill bugs for more than 6 h each. An example of a walking pattern in the T-maze is shown in Fig. 1.

Fig. 1 Trajectory of an individual's gait.

When the turns are repeated regularly, alternating left and right, the pill bug is considered to move straight. Conversely, if the same turn is repeated, such as right and right, it is considered to have changed direction.

In this classification of gait patterns, the pill bug is considered to decide whether to continue or abort straight-ahead movement each time it encounters a T-intersection. The straight-line distance l was calculated using the method shown in Fig. 2. Using this method, time-series data of the straight-line distance l for each individual were obtained.

Fig. 2 Sample calculation of step length *l*. The black polygonal line with the arrow represents a turn; L represents a left turn, R a right turn. The red line represents an approximate linear movement. The L-R-L-R pattern shown in this figure represents linear movement with a step length of 4 (l=4).

Results

Figure 3 shows an example of a discrete case, that is, the GE represented by equation (28). Figure 3(a) and 3(b) show the cases of m=1.0, and m=0.01, respectively. Figure 3(a) shows a single logarithmic graph with the vertical axis on a logarithmic scale and Figure 3(b) shows a double logarithmic graph with both axes on a logarithmic scale. In these figures, the GE for the case $\beta = 0.5, 1.0, 2.0$ is shown. In Fig. 3(a), the exponential approximation curve is shown, and in Fig. 3(b), the power approximation curve is shown. From the figure, we can see that the GE for m=1.0, can be approximated by an exponential distribution with an exponent -β. Conversely, the GE for m = 0.01 can be approximated by the power law distribution with exponent –(β+1).

Fig. 3 Examples of GE. (a) For m=1.0, the GEs are shown for β=0.5, 1.0 and 2.0. The vertical axis is shown logarithmically. The exponential approximation curves are also shown. (b) For m=0.01, the GE for β=0.5, 1.0 and 2.0 are shown. Both axes are shown logarithmically. The power approximation curves are also shown.

Figure 4 shows examples of walking data for three individual pill bugs. Figure 4(a) shows the time series of the step length of subject 4 in the experiment of Shokaku et al [3]. Figure 4(b) shows the CCDF of the step length. Figures 4(c) and 4(d) show the data for subject 15, and Figures 4(e) and 4(f) show the data for subject 14. Figures 4(b), (d), and (f) also show the results of fitting the CCDF of the GE model expressed in equation (30) to the observed data. Figures 4(b), 4(d), and 4(f) are double logarithmic graphs with both axes displayed in logarithmic form. Note that in these figures, $P\left(\hat{l}_{\min}\right) = 1$ is based on the definition of equation (30).

Fig. 4 Step length data for three individuals. (a) Step length time series for individuals of subject 4. (b) CCDF of subject 4. $\hat{l}_{\min} = 3, \hat{l}_{\max} = 30, m = 0.01, \beta = 1.68$ (c) Step length time series for individuals of subject 15. (d) CCDF of subject 15. $\hat{l}_{\min} = 10, \hat{l}_{\max} = 81, m = 0.24, \beta = 0.82$ (e) Step length time series for individuals of subject 14. (f) CCDF of subject 14. $\hat{l}_{\min} = 7, \hat{l}_{\max} = 127, m = 0.44, \beta = 0.42$

Figure 5 shows the relationship between the autocorrelation coefficient $\bar{r}$ of the time-series data of step length and the shape parameter m when the GE fits the frequency distribution of each individual's step length.

Fig. 5 Relationship between shape parameters and autocorrelation coefficients. (a) Scatter plots between shape parameters and autocorrelation coefficients. The regression line is also shown. (b) Box plot for the case of grouping individuals with m=0.01 and m>0.01. (c) Correlogram for each group. The vertical axis represents the mean value of the autocorrelation coefficient of the individuals in the group. The error bars represent the standard errors.

The autocorrelation coefficient shown on the vertical axis represents the average value from $r(1)$ to $r(100)$. In calculating the shape parameter m, only individuals with $\hat{l}_{\max} - \hat{l}_{\min}$ value of 5 or higher were included in the analysis. The autocorrelation coefficients were calculated from 1 to 100 for the time lag, and only individuals with more than 200 time-series data were included in the analysis. A total of 27 individuals were analyzed. The mean ± standard deviation (SD) of the number of time-series data of the step lengths of these individuals was 601.22 ± 285.77. The minimum and maximum values of the data were 213 and 1244, respectively. Figure 5(a) shows a scatter plot of the shape parameters and autocorrelation coefficient. There was no significant correlation between the two parameters (r=-0.47, p =0.014, n=27). Figure 5(b) is a box plot showing the autocorrelation coefficients for each group when the population was divided into two groups: Group 1 (n=19) with m=0.01 and Group 2 (n=8) with m>0.01. The Wilcoxon rank-sum test revealed a significant difference between the two groups (p = 4.05×10^{-5}, W = 145). Figure 5(c) shows the correlogram for each group. The horizontal axis represents the time lag τ. The vertical axis represents the average autocorrelation coefficient for the τ of each individual in each group. The error bars represent the standard error.

Figure 6 shows the relationship between the GE shape parameter m and exponent β for the 27 individuals described above. Figure 6(a) shows a scatter plot for both. There was a significant negative correlation between the two (r=-0.67, p $=1.2\times10^{-4}$, n=27). Figure 6(b) contains a box plot showing the exponent of the GE for each group. The Wilcoxon rank-sum test showed that there was a significant difference between them (p = 9.2×10^{-4}, W = 135).

Fig. 6 Relation between shape parameters and exponent parameters. (a) Scatter plot of the shape parameter and the exponent parameter. The regression line is also shown. (b) Box plot for the case of grouping individuals with m=0.01 and m>0.01.

Discussion

This paper proposes a generalized distribution that includes exponential and power law distributions as special cases. By using this approach, a model can be created that better fits the observed data than the exponential or power law distributions, that is, a model with a higher likelihood. However, this distribution contains two parameters while the exponential and power law distributions only have one parameter. The model most suitable for the relevant data must be determined comparatively by using AICw that considers both likelihood and the number of parameters of the model.

The proposed model handles the intermediate distribution between the exponential and power law distributions. We defined the change rate $\gamma(l)=\beta l^{m-1}$ as shown in equation (15) to connect the exponential and power law distributions. However, the change rate has countless definitions. Therefore, it is necessary to verify the validity and suitability of this definition in the future.

In this study, the proposed GE was applied to the walking data of pill bugs. A significant difference resulted between the autocorrelation coefficients of Group 1, which followed an approximate power law distribution with a shape parameter of m=0.01, and Group 2, which followed the other distributions with shape parameters of m>0.01, as shown in Fig. 5(b). However, this difference is nontrivial. For example, if we randomly shuffle the order of the time-series data as shown in Fig. 4 (a), the time dependence disappears, but the value of the shape parameter is unchanged because the probability distribution, as shown in Fig. 4 (b), is not affected by the shuffling.

As equation (15) shows, the smaller m is, the smaller the change rate becomes as the step length increases. Conversely, the smaller the value of m, the higher is the probability that the step length will be further elongated when the step length increases. This means that when m is small, the occurrence of a long step length becomes more frequent.

As shown in Fig. 6(a), there is a negative correlation between the shape parameter and the exponent parameter of the GE. Otherwise expressed, the exponent parameter tends to increase as the shape parameter decreases. As equation (15) shows, when the exponent parameter increases, the overall change rate increases, and the frequency of the short step length increases. Thus, individuals with small shape parameter values can be said to have a relatively higher frequency of short and long step lengths than those with intermediate step lengths.

Ross et al. [24] demonstrated that in human hunting behavior, the mode of exploration changes depending on encounters with prey. In particular, they indicated that in response to encounters, hunters more tortuously search areas of higher prey density and spend more of their search time in such areas; however, they adopt more efficient unidirectional, inter-patch movements after failing to encounter prey soon enough. This type of search behavior is called an area-restricted search (ARS) [24,25]. In ARS, searches with short travel distances within patches are combined with searches with long travel distances between patches, so there may be a tendency for relatively short and long straight distances to appear more frequently than intermediate straight distances, that is, distributions with small shape parameters may be more likely to appear. In addition, the time dependence of the step length may appear because the search within a patch continues for a while after encountering the food, or conversely, the search between patches continues for a while when the food is not found. It may be that the power law distribution and time dependence tend to appear simultaneously when the search between different levels is combined hierarchically, such as intra-patch and inter-patch searches.

The result of the significant difference between the autocorrelation coefficients of Group 1 and Group 2 is consistent with the result of Wang et al. [13], who found time dependence in the time-series data of step length when the frequency distribution of the step length follows a power law distribution. However, it is unclear why the shape parameter is associated with the time dependence. The shape parameter of the distribution takes into account the history of the distance traveled in a straight line, that is, how long the same process has lasted when elongating the straight-line distance, and is related to the process within single straight-line behavior. Conversely, the time dependence of the time-series data of straight-line distance is associated with the relationship between multiple straight-line behaviors. In the future, why this correlation is observed between the two, must be clarified theoretically and experimentally.

It is also unclear why this association was observed in pill bugs and may have a completely different cause than in humans. The question whether this relationship also manifests in the migratory behavior of animals other than pill bugs requires further research.

Acknowledgments

This research was partially supported by the Center of Innovation Program of the Japan Science and Technology Agency (JST). This work was supported by JSPS KAKENHI, Grant Number JP21K12009.

References

1. Harris TH, Banigan EJ, Christian DA, Konradt C, Wojno EDT, Norose K, et al. Generalized Lévy walks and the role of chemokines in the migration of effector CD8+ T cells. Nature. 2012;486: 545–548. DOI: 10.1038/nature11098.
2. Ariel G, Rabani A, Benisty S, Partridge JD, Harshey RM, Be'Er A. Swarming bacteria migrate by Lévy walk. Nat Commun. 2015;6: 8396. DOI: 10.1038/ncomms9396.
3. Shokaku T, Moriyama T, Murakami H, Shinohara S, Manome N, Morioka K. Development of an automatic turntable-type multiple T-maze device and observation of pill bug behavior. Rev Sci Instrum. 2020;91: 104104. DOI: 10.1063/5.0009531.
4. Humphries NE, Queiroz N, Dyer JRM, Pade NG, Musyl MK, Schaefer KM, et al. The environmental context explains the Lévy and Brownian movement patterns of marine predators. Nature. 2010;465: 1066–1069. DOI: 10.1038/nature09116.
5. Humphries NE, Weimerskirch H, Queiroz N, Southall EJ, Sims DW. Foraging success of biological Lévy flights recorded in situ. Proc Natl Acad Sci U S A. 2012;109: 7169–7174. DOI: 10.1073/pnas.1121201109.
6. Raichlen DA, Wood BM, Gordon AD, Mabulla AZP, Marlowe FW, Pontzer H. Evidence of Lévy walk foraging patterns in human hunter–gatherers. Proc Natl Acad Sci U S A. 2014;111: 728–733. DOI: 10.1073/pnas.1318616111.
7. Sims DW, Southall EJ, Humphries NE, Hays GC, Bradshaw CJA, Pitchford JW, et al. Scaling laws of marine predator search behavior Nature. Nature. 2008;451: 1098–1102. DOI: 10.1038/nature06518.
8. Jansen VA, Mashanova A, Petrovskii S. Comment on "Lévy walks evolve through interaction between movement and environmental complexity". Science. 2012 Feb 24;335(6071): 918; author reply: 918. doi: 10.1126/science.1215747, PMID: 22362991.

9. White EP, Enquist BJ, Green JL. On estimating the exponent of power-law frequency distributions. Ecology. 2008 Apr;89(4): 905-912. doi: 10.1890/07-1288.1. Erratum in: Ecology. 2008 Oct;89(4): 905–912. DOI: 10.1890/07-1288.1, PMID: 18481513.
10. Clauset A, Shalizi CR, Newman MEJ. Power-Law Distributions in Empirical Data. In SIAM Rev. 2009;51(4): 661–703. DOI: 10.1137/070710111.
11. Edwards AM, Phillips RA, Watkins NW, Freeman MP, Murphy EJ, Afanasyev V, et al. Revisiting Lévy flight search patterns of wandering albatrosses, bumblebees and deer. Nature. 2007 Oct 25;449(7165): 1044-1048. doi: 10.1038/nature06199, PMID: 17960243.
12. Shinohara S, Okamoto H, Manome N, Gunji PY, Nakajima Y, Moriyama M, et al. Simulation of foraging behavior using a decision-making agent with Bayesian and inverse Bayesian inference: Lévy and Brownian walk-like search patterns derived from differences in prey distributions. bioRxiv. 2021. doi: 10.1101/2021.06.08.447450.
13. Wang XW, Han XP, Wang BH. Correlations and scaling laws for human mobility. PLOS ONE. 2014;9: e84954. DOI: 10.1371/journal.pone.0084954.
14. Rhee I, Shin M, Hong S, Lee K, Kim SJ, Chong S. On the Levy-walk nature of human mobility. IEEE ACM Trans Netw. 2011;19: 630–643. DOI: 10.1109/TNET.2011.2120618.
15. Zhao K, Musolesi M, Hui P, Rao W, Tarkoma S. Explaining the power-law distribution of human mobility through transportationmodality decomposition. Sci Rep.: 9136. Sci Rep. 2015;5: 9136. https://doi.org/10.1038/srep09136.
16. Weibull W. A Statistical Distribution Function Of Wide Applicability. J Appl Mech. 1951;vol. 18: 293–297. doi:10.1115/1.4010337.
17. Mingw. Available: http://www.mingw.org/. [Accessed 23 January 2021].
18. Qt. Available: https://www.qt.io/. [Accessed 23 January 2021].
19. The Comprehensive R Archive Network. Available: Cran.r-project.org/. (Accessed 15 July 2020).

20. Moriyama T, Migita M, Mitsuishi M. Self-corrective behavior for turn alternation in pill bugs (*Armadillidium vulgare*). Behav Processes. 2016;122: 98-103. DOI: 10.1016/j.beproc.2015.11.016.

21. Hughes RN. Mechanisms for turn alternation in woodlice (Porcellio scaber): The role of bilaterally asymmetrical leg movements. Anim Learn Behav. 1985;13: 253-260. DOI: 10.3758/BF03200018.

22. Jander R. Ecological aspects of spatial orientation. Annu Rev Ecol Syst. 1975;6: 171-188. DOI: 10.1146/annurev.es.06.110175.001131.

23. Moriyama T. Decision-making and turn alternation in pill bugs (*Armadillidium vulgare*). Int J Comp Psychol. 1999;12: 153-170.

24. Ross CT, Winterhalder B. Evidence for encounter-conditional, area-restricted search in a preliminary study of Colombian blowgun hunters. PLOS ONE. 2018;13: e0207633. DOI: 10.1371/journal.pone.0207633.

25. Hills TT, Kalff C, Wiener JM. Adaptive Lévy Processes and Area-Restricted Search in Human Foraging. PLOS ONE. 2013;8(4): e60488. https://doi.org/10.1371/journal.pone.0060488.

471

Fig. 1 Trajectory of an individual's gait.

472

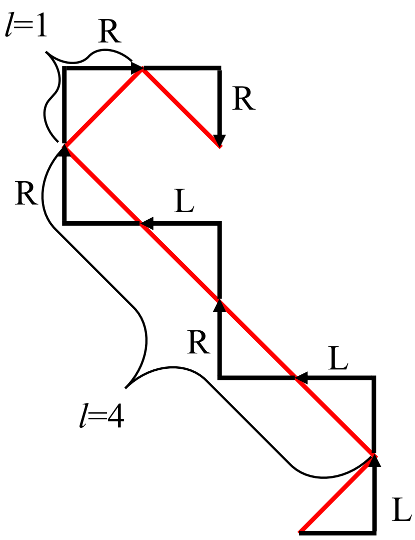

Fig. 2 Sample calculation of step length *l*. The black polygonal line with the arrow represents a turn; L represents a left turn, R a right turn. The red line represents an approximate linear movement. The L-R-L-R pattern shown in this figure represents linear movement with a step length of 4 (*l*=4).

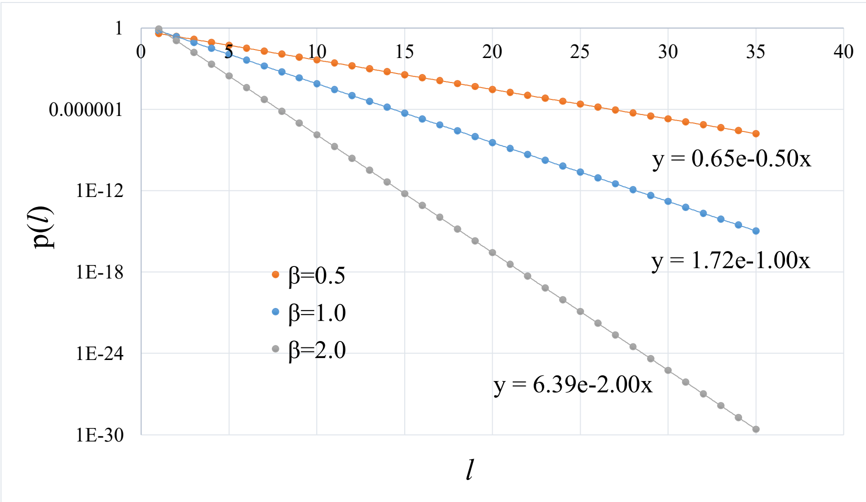

(a)

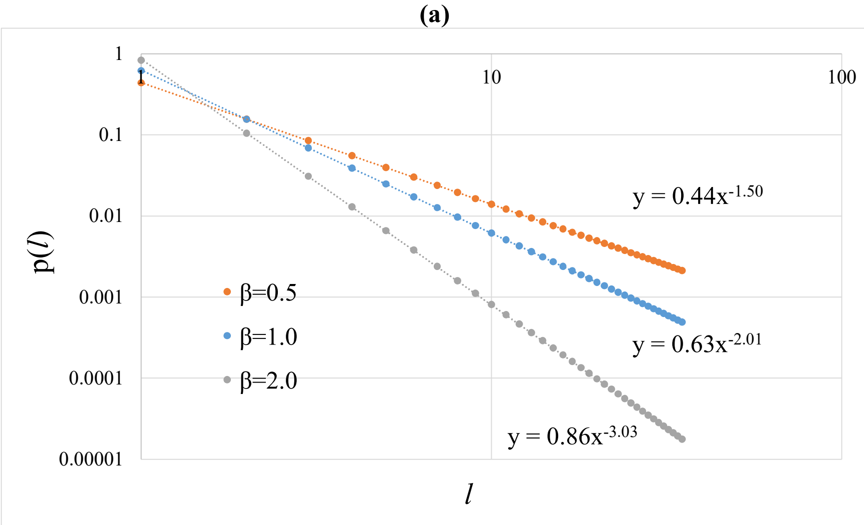

(b)

Fig. 3 Examples of GE. (a) For m=1.0, the GEs are shown for β=0.5, 1.0 and 2.0. The vertical axis is shown logarithmically. The exponential approximation curves are also shown. (b) For m=0.01, the GE for β=0.5, 1.0 and 2.0 are shown. Both axes are shown logarithmically. The power approximation curves are also shown.

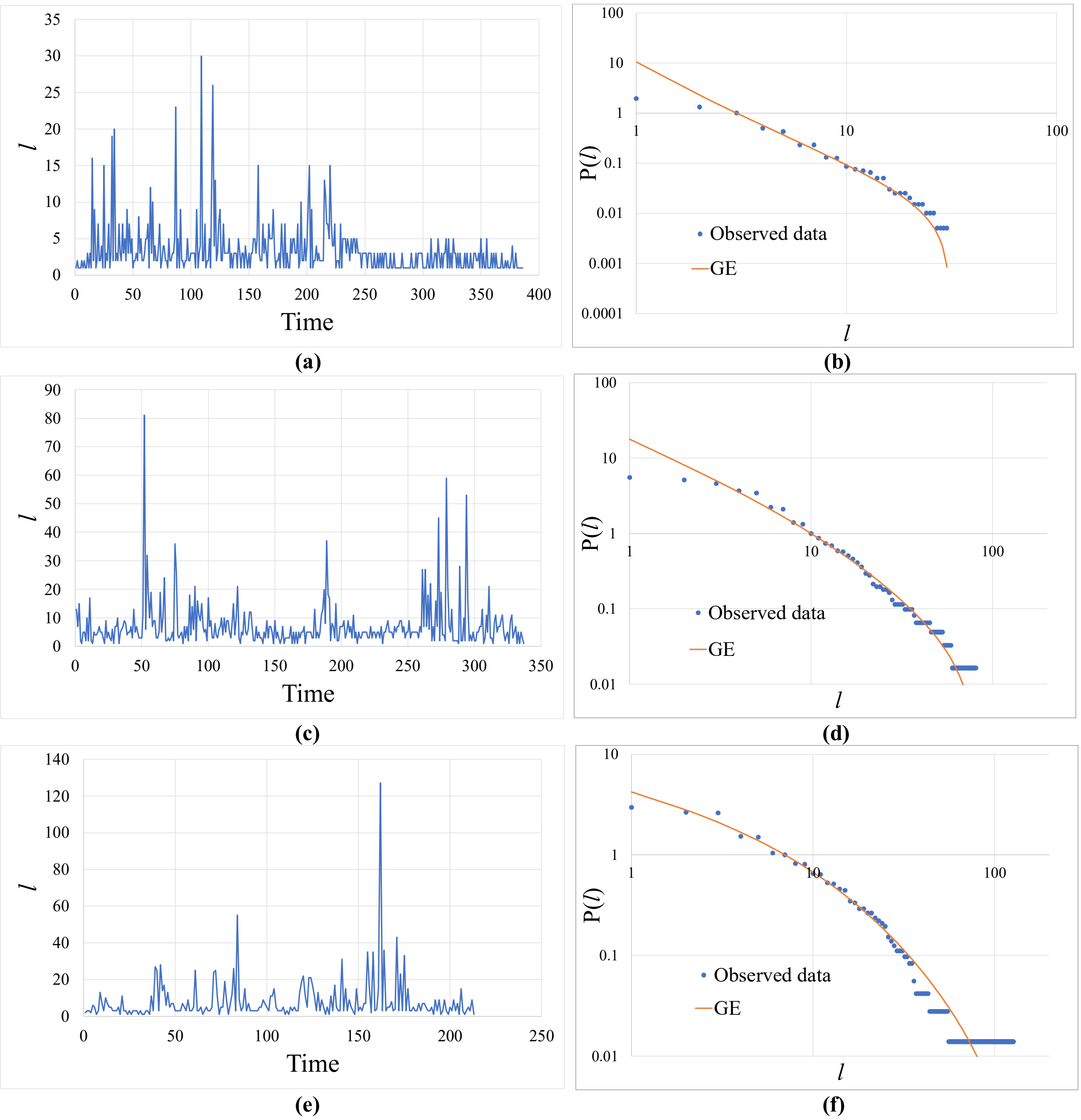

Fig. 4 Step length data for three individuals. (a) Step length time series for individuals of subject 4. (b) CCDF of subject 4. $\hat{l}_{\min} = 3, \hat{l}_{\max} = 30, m = 0.01, \beta = 1.68$ (c) Step length time series for individuals of subject 15. (d) CCDF of subject 15. $\hat{l}_{\min} = 10, \hat{l}_{\max} = 81, m = 0.24, \beta = 0.82$ (e) Step length time series for individuals of subject 14. (f) CCDF of subject 14. $\hat{l}_{\min} = 7, \hat{l}_{\max} = 127, m = 0.44, \beta = 0.42$

476

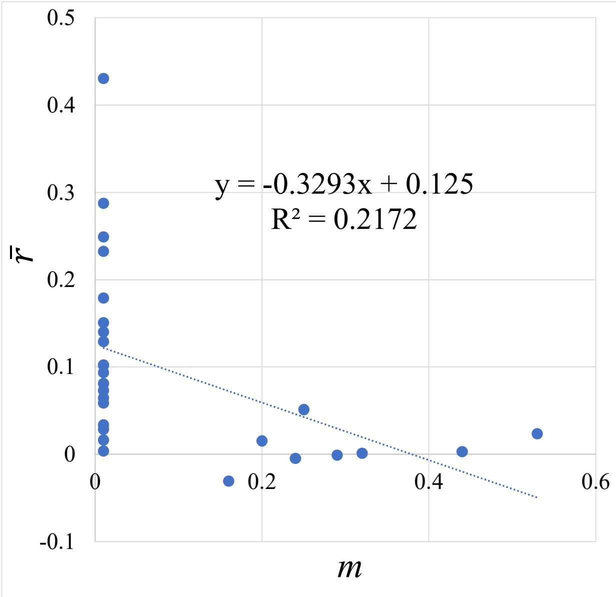

0.5
0.4
0.3
0.2
0.1
0
-0.1
0
0.2
0.4
0.6
$\bar{r}$
m
y = -0.3293x + 0.125
R² = 0.2172

(a)

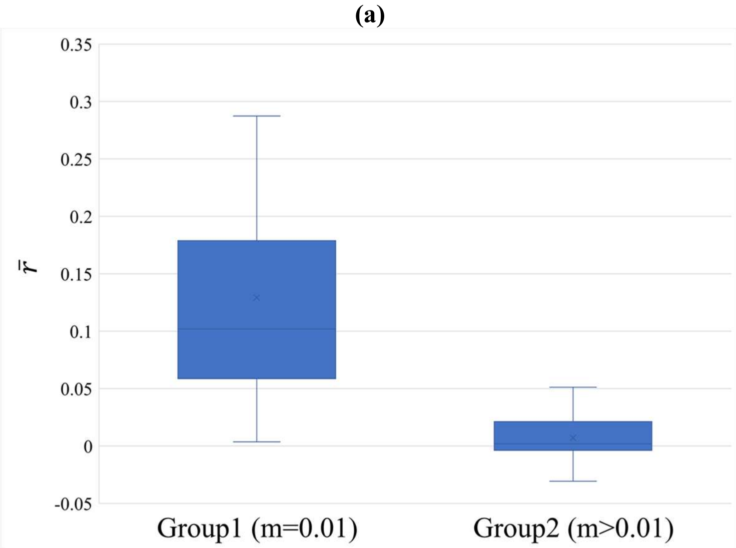

0.35
0.3
0.25
0.2
0.15
0.1
0.05
0
-0.05
$\bar{r}$
Group1 (m=0.01)
Group2 (m>0.01)

(b)

477

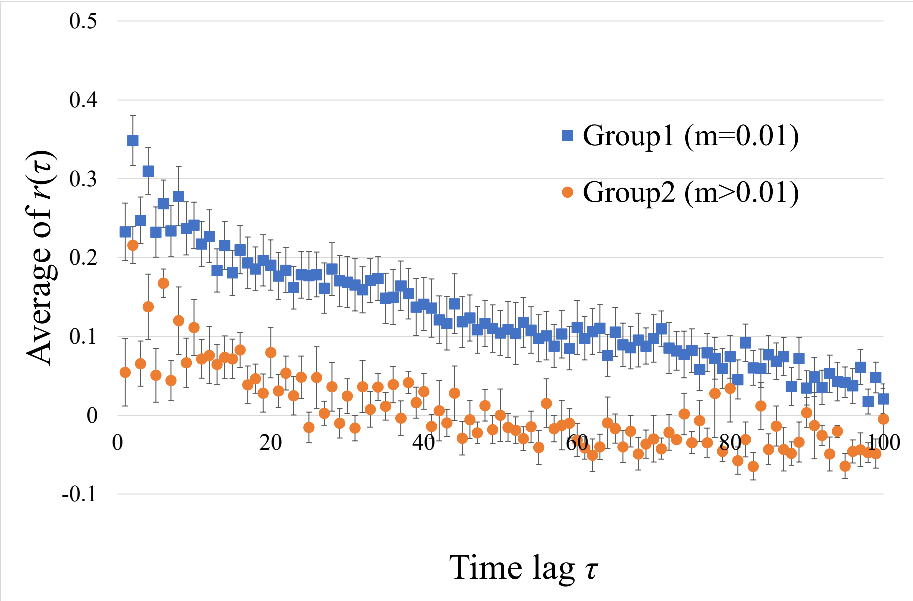

(c)

Fig. 5 Relationship between shape parameters and autocorrelation coefficients. (a) Scatter plots between shape parameters and autocorrelation coefficients. The regression line is also shown. (b) Box plot for the case of grouping individuals with m=0.01 and m>0.01. (c) Correlogram for each group. The vertical axis represents the mean value of the autocorrelation coefficient of the individuals in the group. The error bars represent the standard errors.

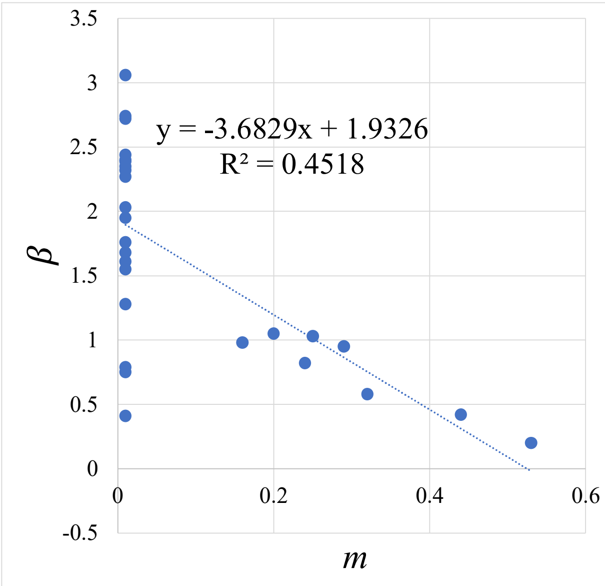

(a)

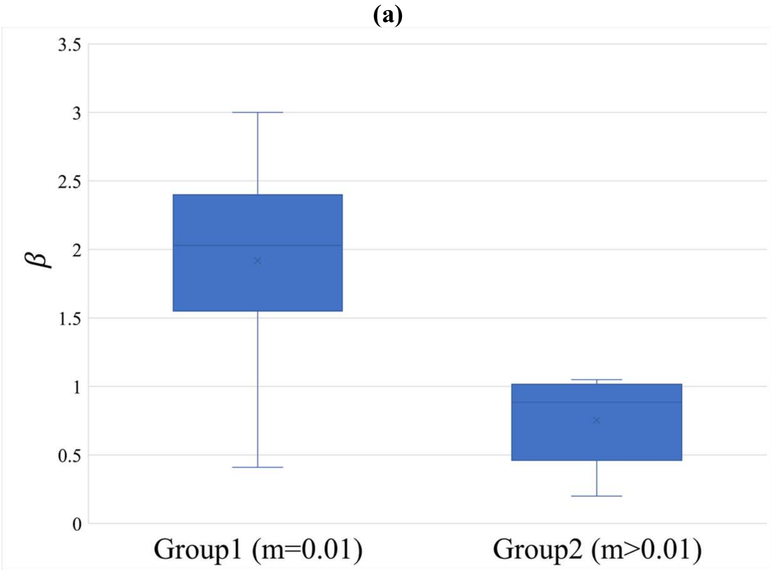

(b)

Fig. 6 Relation between shape parameters and exponent parameters. (a) Scatter plot of the shape parameter and the exponent parameter. The regression line is also shown. (b) Box plot for the case of grouping individuals with m=0.01 and m>0.01.